Fractionalized phase in an $XY-Z_2$ gauge model

R. D. Sedgewick,* D. J. Scalapino,† and R. L. Sugar‡
Department of Physics, University of California, Santa Barbara, California 93106
(Received 8 January 2001; revised manuscript received 15 May 2001; published 8 January 2002)

We study a model with fractional quantum numbers using Monte Carlo techniques. The model is composed of bosons interacting though a Z_2 gauge field. We find that the system has three phases: a phase in which the bosons are confined, a fractionalized phase in which the bosons are deconfined, and a phase in which the bosons are condensed. The deconfined phase has a ''topological'' order due to the degeneracy in the ground state of the gauge field. We discuss an experimental test proposed by Senthil and Fisher that uses the topological order to determine the existence of a deconfined, fractionalized phase.

DOI: 10.1103/PhysRevB.65.054508 PACS number(s): 74.25.Dw, 75.10.Hk, 05.10.Ln, 02.70.Ss

I. INTRODUCTION

A theoretical framework for constructing model many-body systems that can exhibit phases with fractionalized quantum numbers has been proposed by Senthil and Fisher.[1] Here, we report results obtained from a numerical simulation of one such model and examine a recently proposed experimental test for detecting the fractionalized phase.[2,3]

The quantum many-body model that we will study consists of ''chargons'' coupled to a fluctuating Z_2 gauge field in two spatial dimensions. It was obtained by Senthil and Fisher by considering the special case of *s*-wave pairing with an even number of electrons per unit cell, and integrating out the spinon degrees of freedom. This model has the advantage of being straightforward to simulate, while allowing a test of some of the underlying ideas associated with the fractionalized phases. The Hamiltonian for the 2D quantum lattice has the form

$$H=-J\sum_{\langle ij\rangle}\sigma_{ij}^{z}(b_i^{\dagger}b_j+\text{H.c.}) +A\Sigma n_i^2-K\sum_{\square}\left[\prod_{\square}\sigma_{ij}^{z}\right]-h\sum_{\langle ij\rangle}\sigma_{ij}^{x}, \qquad (1)$$

where the chargon creation operator is $b_i^{\dagger}=e^{i\hat{\phi}_i}$ and n_i is conjugate to $\hat{\phi}_i$ so that $[\hat{\phi}_i,n_j]=i\delta_{ij}$. The gauge field operator on the link between nearest-neighbor sites i and j is σ_{ij}^{z}, and $\Pi_{\square}\sigma_{ij}^{z}$ is the product of gauge operators around a plaquette. The sum $\langle ij\rangle$ is over nearest neighbor sites on the 2D spatial lattice. A ''vison'' excitation consists of a plaquette for which $\Pi_{\square}\sigma_{ij}^{z}$ is equal to -1. Visons are always joined in pairs by a string of plaquettes with two links flipped relative to the rest of the links in the vicinity. A schematic example of this is shown in Fig. 1(a). Here and in the text, we have taken the flipped links to have $\sigma_{ij}^{z}=-1$ for definiteness.

For the purpose of carrying out simulations, we work with the 3D (two space and one Euclidean time) classical action associated with the Hamiltonian of Eq. (1),

$$S=-J\sum_{\langle ij\rangle}\sigma_{ij}\cos(\phi_i-\phi_j)-K\sum_{\square}\left[\prod_{\square}\sigma_{ij}\right]. \qquad (2)$$

This action has an XY angular variable ϕ_i corresponding to the eigenvalue of the operator $\hat{\phi}_i$ and a Z_2 gauge field $\sigma_{ij}=\pm 1$ corresponding to the eigenvalue of the operator σ_{ij}^{z}. Here, $\langle ij\rangle$ indicates all nearest neighbor sites on the 3D lattice. This action has rotational symmetry as well as a local Z_2-gauge symmetry in which ϕ_i at a site transforms to $\phi_i+\pi$ and all of the σ_{ij} gauge fields linked to the ith site change sign. As discussed in Ref. 1, this model is expected to have the type of phase diagram illustrated in Fig. 2. Both the gauge field σ_{ij} and the XY field ϕ_i are disordered in region I when J and K are small. In the 2D quantum version, this corresponds to the fluctuating σ_{ij}^{z} gauge field confining the chargons so that there are no free $b_i^{\dagger}$ excitations, only $(b_i^{\dagger})^2$ excitations. In region III, the XY rotation symmetry is broken, as well as the Z_2 gauge symmetry. This is just the usual XY phase with a finite helicity modulus. Here, chargon pairs $(b_i^{\dagger})^2$ condense to form a superfluid.

Region II corresponds to a ''fractionalized'' (unconfined) phase. We find that the ϕ field is disordered, as in region I, but the Z_2 gauge field is ordered, or equivalently in the quantum version, the visons are gapped.[11] This allows the chargon pairs to ''fractionate,'' and individual $b_i^{\dagger}$ chargon excitations are present in the quantum version. As one enters the superconducting phase, region III, it is the $b_i^{\dagger}$ field that condenses.

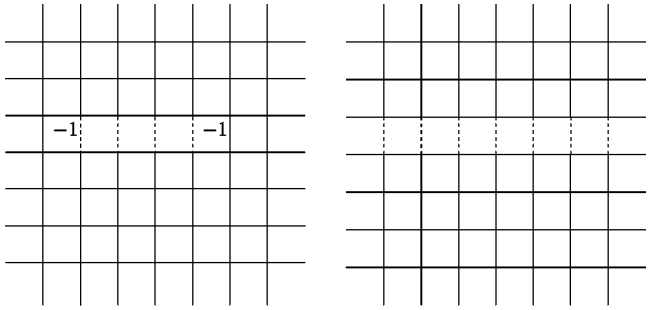

FIG. 1. Schematic representation of the 2D quantum system. Solid lines denote $\sigma_{ij}=1$, dotted lines denote $\sigma_{ij}=-1$. All visons on the lattice are labeled -1.

 ©2002 The American Physical Society

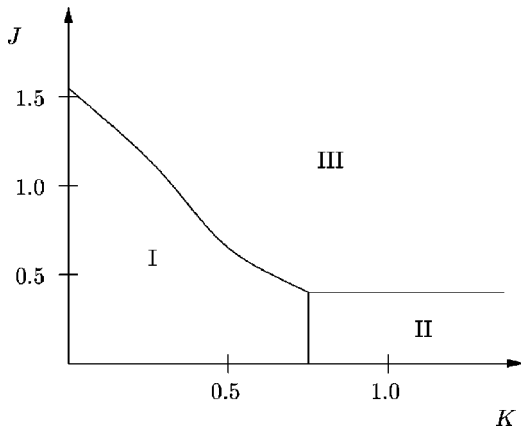

FIG. 2. Phase diagram showing confined phase (I), deconfined phase (II), and boson condensed phase (III).

The fractionalized phase, region II, is characterized by a ''topological'' order. That is, on a manifold with a nontrivial topology, the ground state of the 2D quantum system has a degeneracy that depends upon the topology. With periodic boundary conditions the 2D quantum system has the topology of a torus. A nontrivial topological excitation occurs if a string of plaquettes with two flipped links associated with a vison pair cuts through the torus, as illustrated schematically in Fig. 1(b). In order to minimize the energy, the ϕ field has a discontinuity of $\pi \pmod{2\pi}$ across the flipped links denoted by the dashed lines of Fig. 1(b). Because the ϕ field does not have long-range order in region II, this disturbance dies out within a correlation length, and its energy does not grow with the lattice size. When a vison loop threads the 3D torus used in our simulations, this topological configuration is trapped because the free energy barrier the system must go over to reach the no-vison state grows as the lattice size, L, which goes to infinity in the bulk limit. As proposed by Senthil and Fisher, the existence of this topological order can be probed by driving this system into the superfluid state III, where the ϕ field does have long-range order. In this case, when a trapped vison is present in region II and the system is driven from region II to region III (by, for example, increasing J), the π phase shift in ϕ associated with the vison will induce a circulating current of bosons.[2] Thus, by going into the superconducting phase III one can look for trapped visons by measuring the boson current. If they exist, the trapped visons tell us that we have come from a ''fractionalized'' phase.

Abelian gauge theories have been studied extensively by high-energy physicists since the earliest days of lattice gauge theory.[4] The work most closely related to our own is the study of the Abelian Higgs model with a Z_2 gauge field coupled to an Ising matter field,[5–7] and a $U(1)$ gauge field coupled to an XY-matter field.[6,8,9] Here we study a Z_2 gauge field coupled to an XY field. More recently, an action similar to that of Eq. (2), but with an $O(3)$ matter field, was used by Lammert, Rokhsar, and Toner to study a classical model for nematics.[10]

The existence of three distinct phases in the model we study is consistent with conclusions drawn from the study of more general Abelian Higgs models, in which the Higgs field is not in the fundamental representation of the gauge group.[6] In particular, as pointed out by Senthil and Fisher,[1] each of the phases discussed here has an analogue in the $O(3)$ model of nematics.[10] By contrast, the Z_2 gauge theory coupled to an Ising matter field has only a confined and a deconfined phase with the Higgs and confined phases being analytically connected,[6,7] as is expected in general for Abelian Higgs theories in which the matter field is in the fundamental representation of the gauge group.[6]

In Sec. II, we will discuss Monte Carlo results for the Polyakov loop (the product of σ_{ij} wrapped periodically around the lattice) and the helicity modulus that give us numerical results for the phase diagram. Then in Sec. III, we will discuss visons and the Senthil–Fisher test for fractionalization. Section IV contains our conclusions.

II. PHASE DIAGRAM

Using the 3D Euclidean action, we measure the Polyakov loop and the helicity modulus to find the transitions in both the gauge field and the bosonic field. On our lattices the Polyakov loop provides a useful probe of the gauge field, as we will discuss. The helicity modulus measures the stiffness of the bosonic field to rotating the spins. It can indicate the phase of the boson field, since in our XY spin formulation the superconducting state is characterized by a finite spin stiffness.

It is well known that for $J=0$ the action of Eq. (2) gives rise to a second-order phase transition on an infinite three-dimensional lattice.[4] The confined (strong coupling) phase is characterized by area law behavior of the Wilson loops, and the deconfined (weak coupling) phase by perimeter law behavior. However, on a finite lattice there is a crossover, rather than a *bona fide* phase transition. For the relatively small lattices on which we perform our simulations, measurement of the Polyakov loop provides a convenient way to locate the crossover. A Polyakov loop is the product of a line of σ_{ij} wrapped periodically around the lattice,

$$P_{\hat{\mu}} = \sigma_{ij}\sigma_{jl}\cdots\sigma_{mn}\sigma_{ni}, \tag{3}$$

where all the links are pointing in the $\hat{\mu}$ direction. For strong coupling it vanishes order by order in perturbation theory, and in our simulations we find that it fluctuates about zero, as is seen in Fig. 3. At weak coupling an expansion about the state in which all the σ_{ij} have the same sign gives, to leading order,[4]

$$P = e^{-2Le^{-8K}}, \tag{4}$$

where L is the number of lattice points in the temporal direction. A reference state in which the Polyakov loop has the same magnitude, but opposite sign, can be obtained by the addition of a vison through the torus that flips all the links in the temporal direction between two adjacent time slices. By tracking P in our simulations, we observe the system tunneling between these two degenerate states, as is seen in Fig. 4. On our finite lattice P averages to zero because of cancellations between states in which it takes on positive and negative values, but above the transition the tunneling occurs

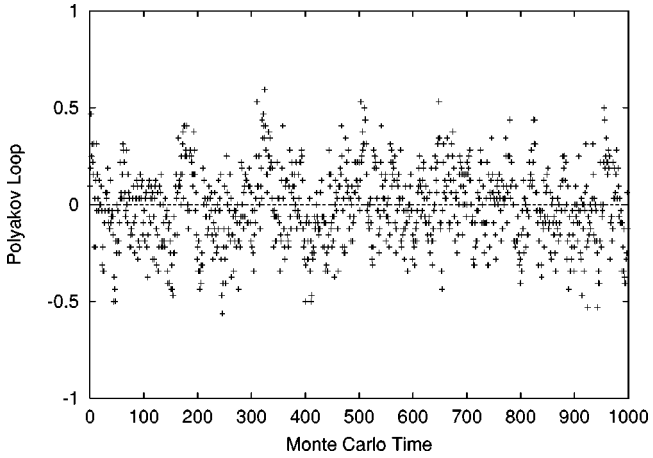

FIG. 3. The average of the Polyakov loop across the lattice as a function of Monte Carlo time for J=0, K=0.69. This is done on an 8^3 lattice using local Metropolis updating.

much less frequently than our period of observation so that we obtain a nonzero average. It follows from Eq. (4) that for $L\rightarrow\infty$ the jump in P goes to zero. However, in our simulations, $L=8$, and the crossover is in the neighborhood of $K=0.7$. For these values the magnitude of the Polyakov loop at the crossover is approximately 0.94. We then measured the Polyakov loop along lines of constant J and K. Figure 5 shows the expectation value of Polyakov loops along lines of constant K. These Monte Carlo measurements were taken using a local Metropolis updating scheme on a lattice with 8^3 sites. We took 150 measurements for each point with each measurement separated by 35 Monte Carlo updates of the lattice. After the measurements at a point are done, J is increased and the system is allowed to equilibrate for 200 Monte Carlo updates. In this case, each run is started with the system completely ordered so that no vison loops get frozen into the system. Figure 6 shows the expectation value of Polyakov loops along lines of constant J. The measurements were taken in the same way with K increased during the run instead of J. Additionally, 500 Monte Carlo steps

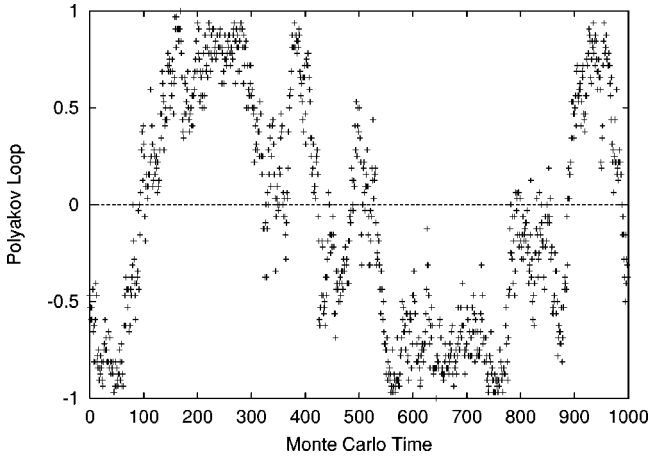

FIG. 4. The average of the Polyakov loop across the lattice as a function of Monte Carlo time for J=0, K=0.73. This is done on an 8^3 lattice using local Metropolis updating.

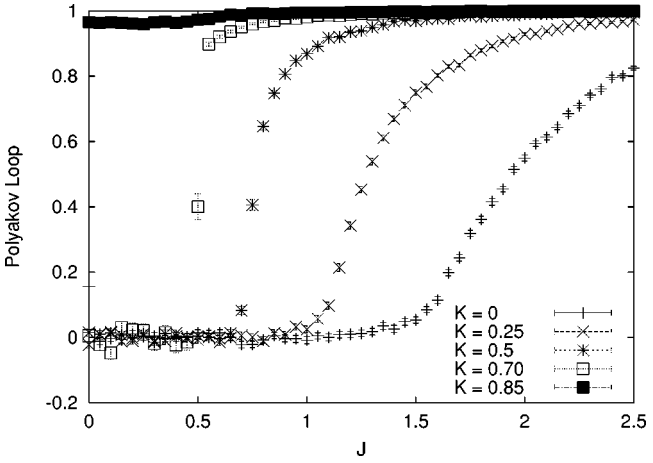

FIG. 5. Expectation value of the Polyakov loop on an 8^3 lattice along lines of constant K. We took 150 measurements at each point with each measurement separated by 35 Monte Carlo steps. The system is allowed to equilibrate for 200 Monte Carlo updates between points.

were used in between measurements to equilibrate. For this figure each run is started from a completely disordered state. When the system enters the deconfined phase (II) from the confined phase (I) it has the opportunity to trap a vison. A trapped vison changes the expectation value of the Polyakov loop from 1 to -1 and accounts for the run with $J=0.3$.

The standard form of the helicity modulus for the XY model is not invariant under the Z_2 gauge transformation. It can be made gauge invariant by inserting factors of the gauge field. This gives a helicity modulus of the form

$$\Upsilon_{\hat{\mu}}/J=\frac{1}{N}\left\langle \sum_{\langle ij\rangle} \sigma_{ij}\cos(\phi_i-\phi_j)(\hat{\epsilon}_{ij}\cdot\hat{\mu})^2\right\rangle - \frac{J}{N}\left\langle\left(\sum_{\langle ij\rangle}\sigma_{ij}\sin(\phi_i-\phi_j)\hat{\epsilon}_{ij}\cdot\hat{\mu}\right)^2\right\rangle, \qquad (5)$$

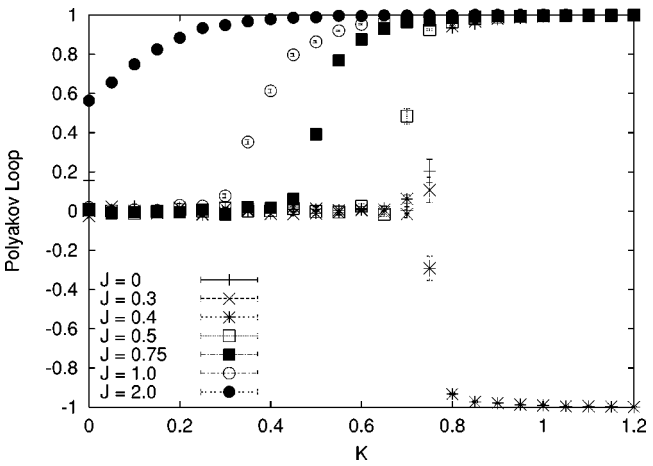

FIG. 6. Expectation value of the Polyakov loop on an 8^3 lattice along lines of constant J. We took 150 measurements at each point with each measurement separated by 35 Monte Carlo steps. The system is allowed to equilibrate for 500 Monte Carlo updates between points. A vison is trapped in the run where $J=0.4$.

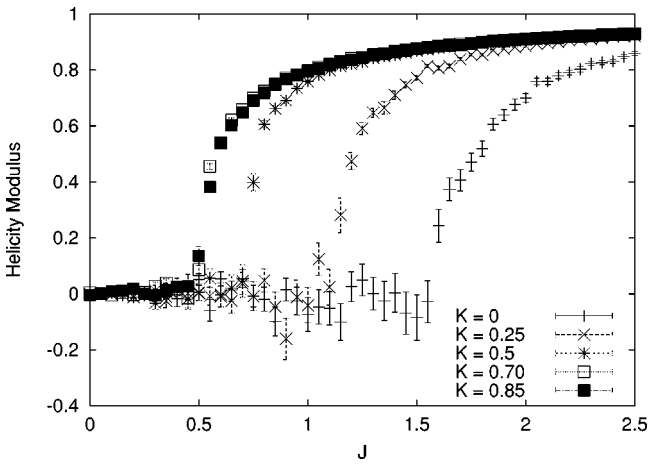

FIG. 7. Expectation value of the helicity modulus on a 8^3 lattice along lines of constant K. We took 150 measurements at each point with each measurement separated by 35 Monte Carlo steps. The system is allowed to equilibrate for 200 Monte Carlo updates between points.

where $\hat{\mu}$ points along the bonds in the $\hat{x}$, $\hat{y}$, or $\hat{z}$ directions and $\hat{\epsilon}_{ij}$ is a unit vector pointing from the ith lattice site to the jth lattice site. Since the helicity modulus measures the stiffness of the spins, it is 0 where the bosons are disordered and finite where the bosons have long-range order.[12] The helicity modulus measured along lines of constant K is shown in Fig. 7. These measurements were taken in the same way as the measurements of the Polyakov loop: 150 measurements at each point separated by 35 Monte Carlo steps between measurements and 200 Monte Carlo measurements between points. The transition is rounded due to finite size effects.

The results found by looking at the expectation value of the helicity modulus and the Polyakov loop were used to construct the phase diagram shown in Fig. 2. The transitions were taken to be when the observable is statistically nonzero. The nature of the transition between the deconfined phase and the confined phase and between the deconfined phase and the condensed phase are understood from studying the Ising model and the XY model, and the boundary between the confining phase and the condensed phase has been studied by Senthil and Fisher.[13] This is a transition at which both the gauge field and the boson field order. This phase transition occurs down to $K=0$ where there is no plaquette term in the action, implying that it is the ordering of the bosons that forces the gauge field to order.

III. VISONS

As discussed in the Introduction, the fractionalized phase II has a topological order caused by the presence of visons threading the torus. These visons are trapped, as previously noted. Senthil and Fisher recently proposed a method for detecting trapped visons by driving the system between the fractionalized phase II and phase III, in which the ϕ field is condensed.[2,3] In our numerical experiments the presence of visons can be determined by observables such as the Polyakov loop that measure the gauge field directly, while in real-world systems this is typically not possible. It is therefore necessary to be able to determine the topological order without observing the gauge field directly. However, as discussed by Senthil and Fisher, the boson field can be used to probe the topology on the lattice in the condensed phase, in which it has long-range order. Antiperiodic boundary conditions generated by a vison threading the torus cause the bosons to gradually twist by $\pm\pi$ from one side of the vison string to the other. This gives rise to a nonzero gauge invariant current,

$$I_{\hat{\mu}} = J\left\langle \sum_i \sigma_{i\,i+\hat{\mu}} \sin(\phi_i - \phi_{i+\hat{\mu}}) \right\rangle, \tag{6}$$

which can be measured. Here $\hat{\mu}$ is a spatial unit vector perpendicular to the vison string. In this way, measuring the gauge-invariant current can determine the topological order of the lattice. Thus, when a single vison string threads the torus we expect a boson current to flow corresponding to the π change in the phase produced by the vison.

In the ordered phase, the fluctuations in the boson phase lead to a renormalization of J,

$$J_r = J\langle \sigma_{i\,i+\hat{\mu}} \cos(\phi_i - \phi_{i+\hat{\mu}}) \rangle. \tag{7}$$

As the bare coupling J increases and one goes deep into the boson condensed phase, the phase fluctuations decrease and J_r/J goes to 1. In a real physical measurement, the quantity entering the circulation or flux is the renormalized coupling J_r, so that a measurement of $I_{\hat{\mu}}$ gives $J_r\pi$. For a finite L^3 lattice we expect that when a vison is trapped and the system is switched into the condensed boson phase III by increasing J, one will find

$$I_{\hat{\mu}}/J_r = \pm L \sin\left(\frac{\pi}{L}\right), \tag{8}$$

which goes to $\pm\pi$ as L goes to infinity.

The lattice is initially prepared at $K=1$ and $J=1$ in the condensed phase with a single vison string threading the torus and a gradual twist of the bosons by π. In a real-world system, this would be achieved by threading an $hc/2e$ magnetic flux quantum through the sample.[2,3] If the system is then moved to the fractionalized phase by decreasing J to 0.25, the boson current disappears, but the vison remains trapped so that the boson current returns with the same magnitude if the system is moved back to the condensed phase. We have done this numerically on an 8^3 lattice using our Euclidean action, with the results shown in Fig. 8. Here we have plotted $I_{\hat{\mu}}/J$ and we see that this ratio is nonzero in the condensed phase, signifying the presence of a vison that remains trapped in the fractionalized phase. For $K=1$ and $J=1$ on an 8^3, lattice J_r/J is measured to be 0.81 so that

$$\frac{I_{\hat{\mu}}}{J} = \pm\frac{J_r}{J} 8 \sin\left(\frac{\pi}{8}\right) \simeq \pm 2.48, \tag{9}$$

in agreement with Fig. 8. Note that the boson current can be either positive or negative reflecting the direction of the gradual twist induced by the vison.

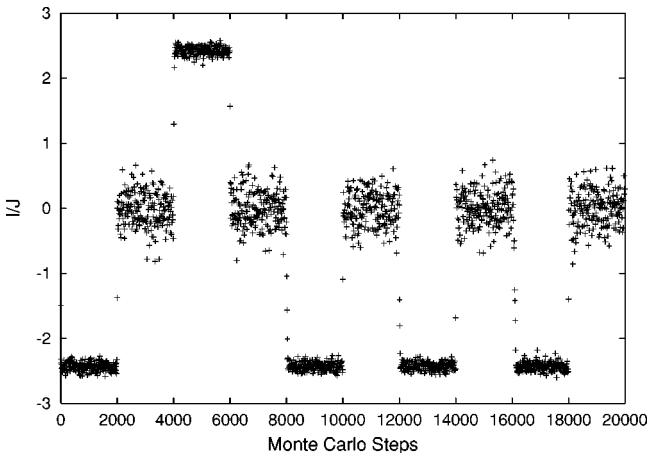

FIG. 8. The 8^3 lattice is moved between the boson condensed phase ($K=1,J=1$) and the deconfined phase ($K=1,J=0.25$) every 2000 Monte Carlo steps. Note that I/J is not $\pm\pi$ in the boson condensed phase due to fluctuations of the bosons and finite size effects as discussed in the text.

If the system with a single trapped vison is moved to a phase without fractionalization, the confined phase I, the vison can escape. For example, at $K=0.5$ and $J=1.5$ we have prepared the system in the condensed phase with a single vison string threading the torus and a boson current, as shown over the first 2000 sweeps in Fig. 9. For $K=0.5$ and $J=1.5$ on an 8^3 lattice J_r/J is measured to be 0.88, so that initially $I_{\hat{\mu}}/J \simeq 2.69$. Then the system is taken into the confined phase I by decreasing J to 0.25 at constant $K=0.5$. When, after another 2000 Monte Carlo steps, the system is taken back into the boson condensed phase III by increasing J to 1.5, the boson current is seen to vanish. This means that the vison that was initially trapped in the condensed phase escaped when J was decreased to 0.25 with $K=0.5$. The boson current remains zero through further cyclings between the phases. This measurement shows that ($J=0.25,K=0.5$) corresponds to a point in the confined phase.

This type of measurement can also be used to determine the line separating the confined and fractionalized phases.

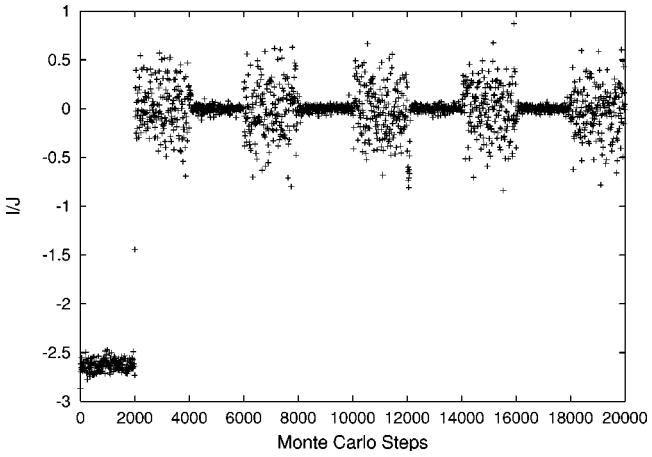

FIG. 9. The 8^3 lattice is moved between the boson condensed phase ($K=0.5,J=1.5$) and the confined phase ($K=0.5,J=0.25$) every 2000 Monte Carlo steps.

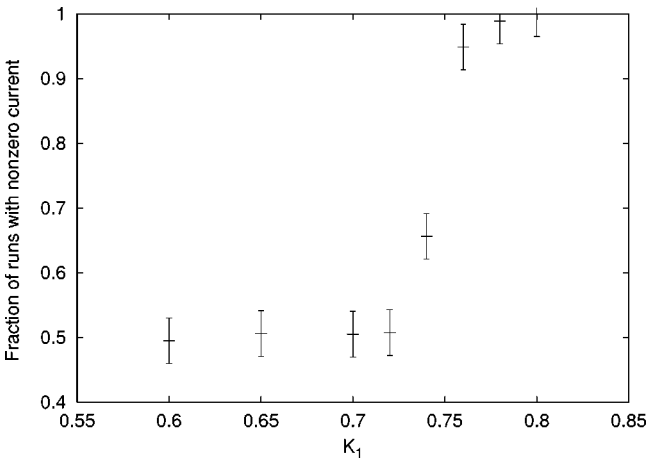

FIG. 10. Fraction of 800 measurements in which an odd number of visons were detected after a system initially prepared in the fractionalized phase with a vison is heated at a constant rate to K_1 and then cooled back to the fractionalized phase. These results are along the line $J_1=0.2$. The existence of an odd number of visons is determined by moving the system to the condensed phase and observing the average bosonic current.

We can determine whether a given point in the phase diagram ($K=K_1,J=J_1$), is in the fractionalized or confined phase by the following set of measurements. We start by equilibrating a trapped vison at the point ($K=1,J=J_1$), which we know to be in the fractionalized phase for sufficiently small J_1. We next decrease K to K_1, equilibrate the system, and then increase K back to 1, where we again equilibrate the system. Finally we move to ($K=1,J=1$), a point at which we know the bosons are condensed. If (K_1,J_1) is in the confined phase, then the trapped vison will escape; however, the system may trap visons when reentering the fractionalized phase. If an odd number of visons are trapped, there will be a nonzero bosonic current in the condensed phase, while if an even number of vison are trapped, no bosonic current will flow in the condensed phase. Thus we expect to find a current in 50% of the runs. On the other hand, if (K_1,J_1) is in the fractionalized phase, then the initial vison will remain trapped, and a nonzero current will be observed in the condensed phase. Figure 10 shows the fraction of 800 trials in which we observed a trapped vison for $J_1=0.2$ and at different values of K_1. The time to equilibrate the lattice in the condensed phase was highly variable because of false energy minima created by trapping several visons. The system has probability 1/2 of trapping an odd number of visons in moving from the confined phase to the fractionalized phase, but when the system is kept in the fractionalized phase the initial vison remains trapped. The transition is rounded due to visons tunneling out of the finite torus close to the transition.

IV. CONCLUSION

In this paper we have reported on an investigation of the XY model coupled to a Z_2 gauge field using Monte Carlo techniques. This model was proposed by Senthil and Fisher for the study of fractionalization. By observing the Polyakov

loop and the helicity modulus, we have determined the structure of the phase diagram of the theory. In addition, we considered an experiment proposed by Senthil and Fisher to determine the existence of a fractionalized phase. Using phase III, in which the bosons are condensed, to measure the existence of a vison, we see that the vison remains trapped in the fractionalized phase. A vison that was trapped in the phase III region is able to escape when the system is taken into the confined phase I.

ACKNOWLEDGMENTS

We would like to thank M.P.A. Fisher and T. Senthil for many insightful discussions. We would also like to thank R. Moessner, S.L. Sondhi and J. Zannan for their helpful comments regarding the Polyakov loop. This work was supported by Department of Energy Grant No. 85-ER-45197, National Science Foundation Grant No. CDA96-01954 and by Silicon Graphics, Inc.

*Electronic mail: rds@physics.ucsb.edu
†Electronic mail: djs@physics.ucsb.edu
‡Electronic mail: sugar@physics.ucsb.edu

[1] T. Senthil and Matthew P.A. Fisher, cond-mat/9910224 (unpublished).
[2] T. Senthil and Matthew P.A. Fisher, cond-mat/0006481 (unpublished).
[3] T. Senthil and Matthew P.A. Fisher, cond-mat/0008082 (unpublished).
[4] J.B. Kogut, Rev. Mod. Phys. **51**, 659 (1979), and references contained therein.
[5] R. Balian, J.M. Drouffe, and C. Itzykson, Phys. Rev. D **11**, 2098 (1975).
[6] E. Fradkin and S.H. Shenker, Phys. Rev. D **19**, 3682 (1979).
[7] M. Creutz, Phys. Rev. D **21**, 1006 (1980).
[8] M. Einhorn and R. Savit, Phys. Rev. D **17**, 2583 (1978); **19**, 1198 (1979).
[9] D.R.T. Jones, J. Kogut, and D.K. Sinclair, Phys. Rev. D **19**, 1882 (1979).
[10] P.E. Lammert, D.S. Rokhsar, and J. Toner, Phys. Rev. Lett. **70**, 1650 (1993).
[11] L. McLerran and B. Svetitsky, Phys. Rev. D **24**, 450 (1981).
[12] Ying-Hong Li and S. Teitel, Phys. Rev. B **40**, 9122 (1989).
[13] T. Senthil and Matthew P.A. Fisher (private communication).